



VICTORIA UNIVERSITY
MELBOURNE AUSTRALIA

Effect of supercritical CO₂ and olive leaf extract on the structural, thermal and mechanical properties of an impregnated food packaging film

This is the Accepted version of the following publication

Cejudo Bastante, C, Cran, Marlene, Casas Cardoso, L, Mantell Serrano, C, Martínez de la Ossa, EJ and Bigger, Stephen W (2019) Effect of supercritical CO₂ and olive leaf extract on the structural, thermal and mechanical properties of an impregnated food packaging film. *Journal of Supercritical Fluids*, 145. pp. 181-191. ISSN 0896-8446

The publisher's official version can be found at
<https://www.sciencedirect.com/science/article/pii/S089684461830528X?via%3Dihub>
Note that access to this version may require subscription.

Downloaded from VU Research Repository <https://vuir.vu.edu.au/38169/>

1 **Effect of Supercritical CO₂ and Olive Leaf Extract on the Structural, Thermal and Mechanical**
2 **Properties of an Impregnated Food Packaging Film**

3 C. Cejudo Bastante^{*a}, M. J. Cran^b, L. Casas Cardoso^a, C. Mantell Serrano^a, E. J. Martínez de la Ossa^a,
4 S. W. Bigger^b

5 ^aChemical Engineering and Food Technology Department, Wine and Agrifood Research Institute
6 (IVAGRO), University of Cadiz, Cádiz, Spain

7 ^bInstitute for Sustainable Industries and Liveable Cities, Victoria University, Melbourne, Australia

8 ^{*}corresponding author: Cristina Cejudo Bastante (cristina.cejudo@uca.es)

9 **Abstract** (150 words)

10 Poly(ethylene terephthalate)/polypropylene (PET/PP) films containing olive leaf extract (OLE) were
11 obtained by supercritical solvent impregnation (SSI) in batch (BM) and semi-continuous (SM) modes.
12 The study focused on the impact of pressure, temperature, CO₂ flow and OLE on the properties of the
13 impregnated films. Thermal analysis of non-impregnated samples revealed a decrease in the
14 crystallinity of PP layer treated at 35 °C and an increase in the T_g of PET treated at 55 °C due to CO₂
15 sorption. In impregnated samples, high pressures caused a decrease in the crystallinity of PP layer,
16 whereas PET layer remained unaffected. Higher pressures favour impregnation in BM, whereas
17 different trends were found for SM impregnations. Although the film properties were not compromised
18 after impregnation, the CO₂ stream used in SM slightly weakened the impregnated films. Overall,
19 conditions of 400 bar and 35°C in BM were favorable for producing highly antioxidant films with minor
20 structural modifications.

21
22
23 **Keywords** (6): PET/PP multilayer film; supercritical impregnation; olive leaf extract; active packaging;
24 film properties

25 **1. Introduction**

26 The demand for minimally processed foods without additives is ever increasing and one of the more
27 innovative alternatives is the inclusion of preservatives in food packaging materials. The use of natural
28 antioxidant compounds (AOs) in packaging films offers some advantages compared to the direct
29 addition of preservatives to the foodstuff. These include the need for lower amounts of active
30 compounds to impart AO activity, the potential for the controlled release to the food matrix, and
31 confining the AO activity to the product surface [1].

32 In the food packaging field, there is usually no single material that has all the requirements for the
33 conservation of a specific product and so the combination of different materials is often used to optimize
34 the packaging. Multilayer films have thus gained attention due to these providing certain mechanical,
35 barrier or heat-sealing properties that monolayer films cannot offer [2, 3]. Multilayer films have been
36 used for creating AO or antimicrobial (AM) packaging using polymers alone or in combination with
37 other materials such as paper or fibers [4-7]. Among them, low- and high-density polyethylene (LDPE
38 and HDPE), ethylene-vinyl acetate (EVA), poly(lactic acid) films (PLA), poly(ethylene terephthalate)
39 (PET) or polypropylene (PP) are commonly used as substrates in active packaging material. In
40 particular, PET has been used in coatings and multilayer formulations for obtaining an oxygen barrier
41 material [8-11], whereas PP has been used in anti-insect and AM packaging material [12, 13].

42 Although procedures such as extrusion or coating have been used traditionally for developing active
43 packaging, supercritical solvent impregnation (SSI) using CO₂ offers numerous advantages compared
44 with other practices due to its mild critical point conditions (31.06 °C and 73.8 bar), high diffusivity,
45 low viscosity and inert nature among other factors [14]. It is also possible to impregnate both non-polar
46 and polar compounds (whether adding low amounts of polar solvents) and control the loading extent by
47 modifying the operating parameters such as pressure, time, temperature or depressurization rate [15].

48 The mild operating temperatures, which do not compromise the stability of the active substance, is very
49 advantageous when compared to other strategies for incorporation of active substances such as thermal
50 extrusion, where the temperatures employed in the film manufacture can exceed 200 °C [8].

51 Additionally, there is no requirement to modify the polymer surface in order to improve adhesion
52 properties that promote the impregnation of compounds [16-19].

53 From an environmental point of view, SSI is considered to be a “green” technique since minimal
54 amounts of polar solvents are required and generally only in cases where the active substances are not
55 well dissolved by the CO₂ [20]. Moreover, solvent-free films are obtained and a final evaporation is
56 usually not required which is advantageous for film integrity. Therefore, SSI is a suitable alternative
57 for the inclusion of an active substance on a polymer matrix after processing. The use of this technique
58 in PET and PP polymers has been previously reported in the literature associated with food, medical
59 and textile fields. For example, Belizón et al. [21] developed a PET/PP multilayer film impregnated
60 with mango extract that was effective in the preservation of lettuce and tangerine. Champeau et al. [22]
61 used polymers such as PP and PET as suture materials that were effectively impregnated with drugs as
62 acetylsalicylic acid or ketoprofen for medical purposes, whereas Herek et al. [23] and Miyazaki et al.
63 [24] used supercritical impregnation for polymer dyeing.

64 Despite the wide applicability of this technique, one potential disadvantage of SSI is the consequences
65 that the severe operational conditions may have on the integrity of the polymer matrix which can include
66 delamination, the appearance of bubbles, and weakness or loss of mechanical properties. Factors such
67 as the impregnation conditions, the presence of the active compound or the supercritical CO₂ (scCO₂)
68 sorption of the polymer can potentially cause damage to the matrix due to the swelling and plasticizing
69 effects directed to the amorphous regions of the polymer [25-27]. This could subsequently alter some
70 chemical and physical characteristics of the films including the morphology, the thermal stability or the
71 mechanical properties [28].

72 The process of SSI consists of three general steps which can be performed using one or two vessels: (i)
73 solubilisation of the active substance in the supercritical phase; (ii) swelling of the polymer matrix in
74 the supercritical phase; and (iii) diffusion of the active compound into the swollen polymer.
75 Depressurization is then performed which facilitates the impregnation of the active compound into the
76 matrix [29, 30]. The most common method of supercritical impregnation is *via* static or batch mode
77 (BM), although some investigators have started to apply a dynamic or semi-continuous mode (SM) in

78 order to improve impregnation efficiency [29, 31, 32]. In BM, the process proceeds with the vessel's
79 outlet closed and the scCO₂ is introduced until the pre-set pressure conditions are reached inside the
80 vessel. In contrast, the SM process involves a stream of scCO₂ at a constant pressure that flows across
81 the impregnation cell continuously. In one example, Ivanovic et al. [33] investigated the BM
82 impregnation of thymol in poly(caprolactone) (PCL) and poly(caprolactone-hydroxyapatite) in a single
83 vessel, by placing the polymers in two different baskets with the extract placed at the bottom.
84 Milovanovic et al. [31] used the same procedure but compared the results with those obtained with an
85 integrated process of extraction-deposition of thyme carried out in two vessels with CO₂ recirculation.
86 Furthermore, Manna et al. [34] successfully impregnated poly(vinyl pyrrolidone) microparticles with
87 ketophen using an SM process with two vessels both working at the same conditions of pressure and
88 temperature.

89 Clearly, a wide range of polymers impregnated with both chemicals and natural extracts using scCO₂
90 have been reported in the literature [35-39]. Among the natural compounds, OLE has been used for
91 food preservation due to its reported AO, antibacterial and antifungal properties [40-44]. Moreover, the
92 olive tree is one of the main crops grown in the Mediterranean basin and is therefore a widely available
93 resource and a by-product of potential interest.

94 The present paper is aimed at reporting the development of an antioxidant PET/PP laminated film
95 impregnated with OLE by the SM and BM processes carried out in one vessel by investigating the effect
96 of scCO₂ flow rate, OLE, and impregnation conditions have over the film properties. To the best of our
97 knowledge, this is the first time that the results obtained by these two impregnation modes have been
98 compared.

99 **2. Material and Methods**

100 **2.1. Chemical Reagents and Raw Materials**

101 Carbon dioxide (99.99%) was purchased from Abello-Linde S.A. (Barcelona, Spain). The reagents
102 required for the determination of the antioxidant activity of the impregnated samples, 2,2-diphenyl-1-
103 picrylhydrazyl (DPPH) reagent and ethanol, were supplied by Sigma-Aldrich (Steinheim, Germany).

104 The polymer film used for impregnation was a multilayer food contact packaging film provided by
105 Technopack Univel S.r.L. (Mortara, Italy). It is comprised of separate layers of PET (12 μm) and PP
106 (50 μm) that are bonded with a urethane adhesive layer. The film thickness specifications were provided
107 by the manufacturer.

108 *Olea europea* leaves were collected from the region of Jaén (Andalucía, Spain) and dried at room
109 temperature and stored in darkness prior to extraction of the OLE. The latter was obtained from 200 g
110 of crushed olive leaf, which was placed in a 1 L reactor. Enhanced solvent extraction was carried out
111 over a period of 2 h at 120 bar and 80 °C using CO₂ and ethanol (1:1) as a co-solvent at a total flow rate
112 of 10 g min⁻¹ following the procedure described by Cejudo Bastante et al. [15].

113 **2.2. Supercritical Impregnation Procedures**

114 The supercritical impregnation equipment was supplied by Thar Technologies (Pittsburgh, PA, USA,
115 model SF500), which includes a vessel (500 mL) coupled with a thermostatic jacket, one high pressure
116 pump with a maximum flow rate of 50 g min⁻¹, CO₂ cylinder, and a back-pressure regulator to control
117 system pressure. For both impregnation methods (BM and SM), the equipment layout is the same but
118 the procedure has some differences to the BM procedure reported previously [15]. In both procedures,
119 1.7 g of plastic film measuring 8 × 30 cm was loaded into the steel supports of the vessel and oriented
120 helically to allow the extract to flow through the layers of the film. Ensuring there was no contact with
121 the film, 15 mL of OLE was loaded in the bottom of the vessel. This amount of OLE was in excess
122 according to a previous study and as such was not considered a limiting factor [15]. During the
123 pressurization step, CO₂ was pumped at a rate of 10 g min⁻¹ until the working pressure was achieved. In
124 the BM process, the vessel outlet was closed and when the required pressure was achieved inside, it
125 was maintained for a period of 1 h. An agitation of 40 rpm was applied to enhance mixing and
126 solubilization of the extract in the supercritical phase. For the SM process, a fresh CO₂ stream was
127 continuously introduced at a flow rate of 2 g min⁻¹, flowing outside the system but maintaining the
128 pressure inside the vessel. The CO₂ enters the vessel from the bottom and exits the vessel at the upper
129 side, creating a forced movement of the CO₂ inside the vessel which effectively agitates the agents.
130 Films were submitted to pressures of 100 and 400 bar and temperatures of 35 and 55°C in both

131 impregnation modes. Once the pressure and temperature conditions were achieved in the vessel,
132 impregnation time commenced and after 1 h of impregnation, a controlled depressurization step was
133 carried out at a rate of 100 bar min⁻¹. In order to evaluate the influence of the operational conditions on
134 the film, samples with no extract were also prepared under the same conditions with films treated with
135 CO₂ only tested in BM. All impregnation conditions were carried out in duplicate.

136 **2.3. Determination of the Antioxidant Loading of OLE in the Film**

137 The DPPH assay is widely used as a method for determining the AO activity of natural extracts in the
138 liquid state [45-47] or immobilized in solids [21, 38], as in the case of impregnated matrices. The
139 reduction of the DPPH reagent in the presence of an impregnated film provides a measure of the AO
140 capacity that the film achieved after impregnation. In this sense, the DPPH reaction was used as an
141 indirect measurement for calculating the loading of the AO compounds introduced by the OLE
142 impregnation of the film. Following the procedure described previously [15], 4 mL of 6 × 10⁻⁵ M DPPH
143 was placed in contact with a known amount of impregnated film. The decrease of the absorbance at 515
144 nm was measured after 2 h of incubation at room temperature and in darkness, when a steady state was
145 achieved. The percentage of inhibition (%I), which represents the concentration of compound that reacts
146 with a given amount of DPPH, was calculated using the following equation:

$$147 \quad \%I = \frac{A_0 - A_i}{A_0} \times 100 \quad (1)$$

148 where A₀ is the initial DPPH absorbance and A_i is the absorbance after 2 h. The relationship between
149 the concentration of OLE (C (μg/mL)) that reacts with the DPPH after 2 h and I% is given by the
150 following empirical equation:

$$151 \quad C = -0.0163 (\%I)^2 + 2.582 (\%I) + 0.2498 \quad (R^2 = 0.999) \quad (2)$$

152 The AO loading of OLE in the film, expressed in terms of mg AO/g film, was calculated from the value
153 of C determined from Equation (2) and the mass of film used in the reaction.

154 **2.4. Structural Analysis using FTIR**

155 Analyses of film surfaces were performed using a Perkin Elmer Frontier FTIR spectrophotometer
156 (Waltham, USA) fitted with a diamond crystal ATR accessory. Each spectrum of the film surface was
157 the average of 16 scans at a resolution of 4 cm⁻¹ over the frequency range 4000–650 cm⁻¹. All spectra
158 were recorded at 25°C and the background spectrum of the clean ATR crystal was collected similarly
159 and automatically subtracted from the sample spectra. Six measurements were performed for each layer
160 of the film, and each condition was measured in duplicate.

161 **2.5. Thermal Analysis using DSC and TGA**

162 A Mettler Toledo DSC1 instrument was used to study the melting endotherms of the films with samples
163 of 4 to 5 mg of film weighed and encapsulated in 30 µL aluminium pans. Using an empty pan as a
164 reference, thermograms were obtained by heating samples from 35 to 300°C, with heating and cooling
165 rates of 10 °C min⁻¹ and a 50 mL min⁻¹ nitrogen gas flow during the analyses. Single experiments were
166 performed on whole film samples without separating the individual layers and the melting temperature
167 (T_m) and melting enthalpy (ΔH_m) were calculated using STAR^e Evaluation Software (Mettler Toledo,
168 version 11.00). The degree of crystallinity (% X_c) was calculated from the area under the enthalpy of
169 fusion endotherm using the following equation:

$$170 \quad \% X_c = \frac{\Delta H_m}{\Delta H_m^0} \times 100 \quad (3)$$

171 where ΔH_m^0 is the melting enthalpy of 100% crystalline PET (140 J g⁻¹) or PP (207 J g⁻¹) [48]. The
172 values of ΔH_m are normalized by the DSC software with respect to the total mass of the sample added
173 to the DSC crucible. Since the polymer film is a laminated structure, the values of ΔH_m were corrected
174 to consider the mass fraction of each component relative to the total mass of the sample in order to
175 calculate the % X_c for each polymer. The correction factor was derived to account for the density
176 (literature values: PET density 1.38 g cm⁻³ [49]; PP density 0.946 g cm⁻³ [50]) and the thickness of each
177 layer (see Section 2.1). For a two-layered laminated film, the mass fraction of component 1:

$$178 \quad m_1 = \rho_1 \times V_t \quad (4)$$

179 where ρ_1 is the density of component 1 and V_t is the total volume of both component layers which is the
180 product of the area and height of the component films and assuming a unit area, the expression becomes:

181
$$m_t = \rho_1 \times \frac{h_1}{h_1+h_2} \quad (5)$$

182 where h_1 and h_2 are the heights of components 1 and 2 respectively. Since the values of densities and
183 thickness are known and constant, the correction factor for the value of ΔH_m for component 1 is given
184 by:

185
$$\Delta H_{m1} = \Delta H_m / m_t \quad (6)$$

186 A Mettler Toledo TGA/DSC1 instrument was employed to perform the TGA experiments. Samples of
187 4 to 5 mg of film were weighed and placed into 70 μ L alumina crucibles prior to heating from 20 to
188 600 $^{\circ}$ C at 10 $^{\circ}$ C min $^{-1}$ under a nitrogen atmosphere flow rate of 50 mL min $^{-1}$. Data were collected with
189 the Mettler STAR $^{\circ}$ Evaluation software and were then exported to Excel for further processing. The
190 kinetics of thermal decomposition and the apparent activation energy, E_a , were assessed using
191 algorithms described by Bigger et al. [51] .

192 **2.6. Mechanical Property Measurement**

193 The tensile strength (TS), of the impregnated films was measured at 25 $^{\circ}$ C using an Instron Universal
194 Testing Machine model 4301 with a load cell of 5 kN. Six tensile specimens from each sample were
195 prepared by cutting strips measuring 1 \times 12 cm. The initial gauge length was set at 100 mm and during
196 the test, a constant cross-head speed of 100 mm min $^{-1}$ was used. The average TS was calculated using
197 Instron BlueHill Series IX software.

198 **2.7. Statistical Analysis**

199 A series of ANOVA tests were carried out to establish statistical differences among the samples. A
200 *post-hoc* Tukey test at $\alpha = 0.05$ was then performed using STATISTICA 8.0 software.

201

202 **3. Results and Discussion**

203 **3.1. Influence of Operational Conditions on Antioxidant Loading of OLE in the Film**

204 Pressure and temperature are the main factors that influence the solvating capacity and diffusivity of
205 scCO $_2$, and the thermodynamic behaviour of the polymer (swelling and plasticizing effects). This work

206 evaluates the effect of pressure and temperature in the range of 100-400 bar and 35-55°C respectively,
207 on the supercritical solvent impregnation of OLE into PET/PP films. In this case, the AO loading of
208 OLE was calculated by analysing the reduction in the absorbance of the DPPH solution in presence of
209 an impregnated film. This reaction indicates the AO capacity of the film, which is determined by the
210 amount of AO compounds from OLE that have been impregnated. The AO loading of the films
211 impregnated by the SM and BM processes under the different conditions is shown in Figure 1, where
212 statistical differences have been analysed by the Tukey test at $\alpha = 0.05$ of significance.

213 When evaluating the influence of the operational parameters on the loading of impregnated films several
214 factors must be considered including the CO₂-OLE affinity [26] and the OLE-polymer affinity. These
215 are related to the solubility and the partition coefficient, as well as the CO₂-polymer affinity [52] and
216 depend partially on the crystallinity [25] and on the CO₂ sorption capacity of the polymer. These factors
217 are of prime importance when the impregnation process is performed in a single vessel since there is
218 only one set of conditions used for both the solubilisation and impregnation of the active substance.
219 Hence, conditions must be chosen to optimize both the solubilisation of the active substances in the
220 CO₂ and the impregnation efficiency.

221 Samples impregnated by BM at 400 bar generally showed a significantly higher loading than those
222 impregnated at 100 bar. These results are in agreement with a previous study of the BM impregnation
223 of OLE in PET/PP films, where a high concentration of compounds from different families were
224 impregnated at high pressure [53]. In the case of the dyeing process for PET, several authors agree that
225 higher pressures favour the CO₂ sorption with increasing temperatures [54], which could lead to a better
226 swelling and plasticizing effect and eventually a greater diffusion coefficient [23, 55]. Other authors
227 have also reported higher CO₂ sorption on both PET and PP under increasing pressures at a temperature
228 of 40 °C [56, 57]. In contrast, previous work on the same matrix showed different results when mango
229 extract was used in a BM process where better impregnation conditions were obtained at 100 bar and
230 45°C in a multilayer PET/PP film [21]. This indicates impregnation process depends on the
231 modifications of polymer when it is in contact with the CO₂, but also on the type of active compound,
232 and even more when it is a complex mixture of different compounds such as natural extracts.

233 When working in SM, the influence of the impregnation conditions differed to those observed in BM
234 where the opposite conditions offered similar AO loading. Since OLE is a mixture of compounds with
235 different polarities, it is possible that applying the 100 bar and 35°C conditions favoured the
236 impregnation of different compounds than those impregnated at 400 bar and 55°C, providing similar
237 antioxidant capacity levels in both conditions. Conversely, films impregnated at 100 bar and 55°C had
238 the lowest AO loadings because these conditions are unfavourable for both the swelling of the polymers
239 and the solubility power of the scCO₂/ethanol mixture.

240 The influence of the impregnation mode is evident when one compares the AO loadings at 400 bar and
241 35°C that were obtained under the BM and SM processes. Since the vessel outlet is closed in BM, the
242 optimal conditions of impregnation must favour both solubilisation of the extract and plasticizing of the
243 film in order to achieve the highest level of impregnation. This was not the case for the SM, where the
244 scCO₂-OLE affinity would prevail over the OLE-polymer affinity, favouring the drawing or removal
245 of OLE outside the vessel and consequently reducing the film loading. This may explain why films
246 impregnated at 400 bar and 35°C in BM showed statistically higher AO loadings than those impregnated
247 in SM.

248 It was evident that although the SM process did not involve a controlled means of agitation within the
249 system, the uniformity of the film loading improved as suggested by the lower standard deviations of
250 the loadings when compared to the BM process. It is possible that the flow of CO₂ in the reactor during
251 the process assists in the homogenization of the scCO₂ and OLE thereby enhances the impregnation
252 process.

253 **3.2. Structural Analysis of Films by FTIR**

254 **3.2.1. Effect of scCO₂ on Non-impregnated Film**

255 The surface structure of each film layer subjected to each of the scCO₂ treatments was elucidated by
256 FTIR spectroscopy with the peaks normalized at 2919 cm⁻¹ and 1243 cm⁻¹ for the PP and PET layers
257 respectively. When compared to the control film with no treatment, the PP layer of the samples
258 subjected to the high-pressure impregnation conditions showed differences at wavenumbers 3430, 3240

259 (—OH and —NH stretch) and 1646 cm^{-1} (—CH₂=CH₂ stretch) as shown in Figure S2 (supplementary
260 data). These peaks are clearly present in the control film but subsequently diminish upon treatment.
261 They are possibly related to hydroxyl stretching originating from the polyurethane adhesive [58]
262 between the layers. During impregnation, the CO₂ produces a swelling effect which generates mobility
263 of the polymer chains and may subsequently reduce the penetration of the IR beam so that the adhesive
264 is no longer visible. This suggests that the swelling effect may be partially irreversible and/or the
265 ordering of the polymer chains upon depressurization is modified.

266 In the case of the PET layer, analysis of the samples subjected to scCO₂ treatment did not show any
267 discernible differences (see Figure S1 supplementary data). The observed spectra are almost identical
268 except for a slight decrease and broadening of the peak at 1713 cm^{-1} (—C=O carbonyl stretch and/or —
269 NH-CO-O-R urethane stretch) [59], possibly due to hydrogen bonding, which is evident mostly for
270 samples treated at 55°C. The extent of the decrease in the peak intensity is not as significant as that
271 observed in the PP layer which may be due to the higher mobility of the polymer chains and the
272 subsequent rearrangement upon depressurization.

273 Some authors have reported the presence of CO₂ is evidenced by peaks at 2300, 3590 and 3695 cm^{-1}
274 [60, 61] but in the present study, no differences were observed between the control and treated samples
275 at those wavenumbers so it is suggested there is an insignificant amount of CO₂ remaining after the
276 impregnation of the film.

277 **3.2.2. Effect of scCO₂ Impregnation of OLE on Film Structures**

278 Surface FTIR-ATR revealed the presence of functional groups and the possible interactions of these
279 with the film upon the introduction of OLE into the scCO₂ reactor vessel. As shown in Figure 2a,
280 differences in bond vibrations were observed in the PET layer including: hydroxyl vibrations between
281 *ca.* $3000\text{--}3650\text{ cm}^{-1}$ [62], symmetric and asymmetric CH₂ and CH stretching vibrations at 2920 and
282 2851 cm^{-1} [63], >C=O carbonyl stretch and/or urethane stretch —NH-CO—O-R at 1713 cm^{-1} [58, 64,
283 65], —C—O— stretch of ester groups at 1018 cm^{-1} , para-disubstituted benzene stretching at 872 cm^{-1} [66],

284 $-\text{CH}_2$ skeletal vibration at 724 cm^{-1} [67], $-\text{NH}_2$ antisymmetric stretching of urethane at 3430 cm^{-1} , and
285 $-\text{SO}_3\text{H}$ in sulfonic acids at 1280 and 1050 cm^{-1} [59] from the OLE.

286 Compared with the spectrum of the control film, the intensity of the peaks at 3340 , 2920 , 2851 cm^{-1}
287 increased in the presence of OLE which can be explained by the glucose and aromatic rings within the
288 structures of the OLE-impregnated phenols [53] and which, in turn, confirms the presence of the OLE
289 on the surface of the impregnated PET layer. Saroufim et al. [68] suggested that the increased absorption
290 band in the region 3340 - 2850 cm^{-1} is due to the formation of large quantities of polar groups. In the
291 present study, the peaks at 872 and 724 cm^{-1} were also prominent due to the presence of the OLE,
292 although the location and intensity of these peaks did not vary significantly over the operational
293 conditions. It is possible that the OLE is bonded to the film *via* the carbonyl moieties in the OLE, which
294 may explain the decrease in the peak at 1714 cm^{-1} when comparing the impregnated samples with the
295 control film. This result is in agreement with several authors who reported that decreases in this band
296 is due to hydrogen bonding of the carbonyl groups between different compounds and different
297 polymeric matrices including cellulose acetate [69], poly(methyl methacrylate) [70], PVP [34], and
298 contact lens materials [71]. Moreover, the broadening of this peak can also reveal the presence of
299 hydrogen bonding [65], which is favoured when the pressure and temperature are increased during the
300 impregnation process.

301 Champeau et al. [52] described two mechanisms of impregnation depending on the affinity between
302 the active substance and polymer: (i) impregnation, where the affinity is good and hydrogen bonding
303 takes place; and (ii) deposition, where the affinity is poor or non-existent and the compounds are trapped
304 on the polymer. In the present study, it is possible that impregnation occurs within the PET layer, and
305 thus a strong interaction takes place between the OLE and the polymer that is evidenced by the peak at
306 1713 cm^{-1} . In the case of the PP layer, which is mostly comprised of long chains of saturated carbon
307 with no functional groups, it is possible that deposition occurs rather than impregnation, and thus a
308 "physical interaction" takes place which does not result in a reduction of the peak intensities of the
309 samples' spectra compared to the control. This has been suggested previously by Kazarian [26], who
310 reported that methyl groups lack the capacity of CO_2 to form interactions with functional groups.

311 Consequently, the band positions of the OLE in the present study suggest that the apparent new bonds
312 observed on the PP layer are due to the presence of OLE (see Figure 2b). The most intense peak
313 variations are observed in the region of 3500-3000 cm^{-1} which is related to the O-H vibration and $-\text{NH}_2$
314 stretching as previously described, with variations also observed in the range of 1790-1550 cm^{-1} . These
315 results are in agreement with Rojas et al. [72], who reported that the $>\text{C}=\text{O}$ stretching band at 1715 cm^{-1}
316 resulting from the impregnation of LLDPE with 2-nonanone is a combination of smaller bands: non-
317 associated carbonyl groups bound by dipole interactions ($>1680 \text{ cm}^{-1}$), or carbonyl groups that are
318 weakly hydrogen bonded to other compounds (1679–1665 cm^{-1}) or strongly hydrogen bonded to other
319 compounds ($<1664 \text{ cm}^{-1}$). Shao et al. [73] related the stretching vibration of the carbonyl group at 1672
320 cm^{-1} to the benzene ring skeletal vibration at 1625 cm^{-1} , which is in the region of the peak vibrations
321 in the present study and this may confirm the presence of the OLE on the film surface. Similarly, the
322 peaks in the region 1455-1355 cm^{-1} which are related to the $-\text{CH}_2$ skeletal vibration [74], are observed
323 to increase with respect to the film control, which is also observed in the OLE spectrum.

324 Comparison of the FTIR spectra obtained at 400 bar in both PP and PET layers showed that there were
325 no observable differences between the impregnation modes along the wavelength range studied (see
326 Figure 2). The spectra of the samples treated at 400 bar and 55°C in either mode provided the highest
327 relative intensity signals. Conversely, when films were impregnated at 100 bar, the SM spectra signals
328 were slightly increased in both layers compared to those of the BM spectra (Figure S3 and S4). This
329 may be related to the higher AO loading shown previously for the film impregnated at 100 bar and 35°C
330 by SM.

331 It can therefore be suggested that the SM process resulted in more significant differences in the FTIR
332 spectra than the BM process and that the higher pressures and temperatures also resulted in greater
333 changes in OLE interactions. In addition, the PP layer was more significantly affected by structural
334 changes than the PET layer. The observed structural modifications are not necessarily related to changes
335 in AO activity since the type of interaction (i.e. impregnation or deposition) can influence the
336 accessibility of the compounds and the subsequent reaction with the DPPH.

337 **3.3. Thermal Analysis**

338 3.3.1. Differential Scanning Calorimetry

339 All DSC thermograms showed peaks that are typical of PET and PP polymers with the glass transition
340 temperature (T_g), cold crystallization temperature (T_{cc}), and melting temperature of each layer (T_m)
341 observed (see Figures 3A and 3B and Figure S5). The T_g is associated with changes in the amorphous
342 region of polymers which depends on the mobility of the polymer chains; the T_m is determined by the
343 transition of the crystalline regions and is specific to each layer; and the T_{cc} is the transition from
344 amorphous to crystalline states where the molecules may achieve, at a certain stage, freedom of motion
345 enough for ordering themselves spontaneously into a crystalline form [75].

346 The results of the various transitions obtained from the thermograms are summarized in Table 1 and
347 when compared statistically to the results of the control film ($\alpha = 0.05$), some modifications were
348 observed in the cases of samples treated with scCO₂ without impregnation. Samples processed at 35°C
349 resulted in reduced crystallinity of the PP with little effect on the crystallinity of the PET layer.
350 Conversely, when samples were processed at 55°C, PP crystallinity was not affected but the T_g of the
351 PET layer was increased. The crystallinity of PET layer remains almost unaffected by the process since
352 the crystalline regions in the polymer do not significantly influence the T_g phenomenon, which is a
353 property associated primarily with the amorphous regions.

354 Champeau et al. [56] defined two conditions for a polymer to have a high CO₂ sorption: (i) the chain
355 mobility, and (ii) the interactions with CO₂. In the present study, PP and PET only fulfil the condition
356 of low sorption of CO₂. The phenyl groups of PET provide rigidity to the polymer structure and
357 considering that the working temperature remains lower than its $T_{g_{\text{PET}}}$ chain mobility is restricted.
358 However, PP has good chain mobility, and the rearrangement of the chains results in a decrease in the
359 crystallinity. Conversely, the phenyl and carbonyl groups of PET can form specific interactions with
360 CO₂ [76], and as the FTIR analysis also revealed in the present study, these interactions could be
361 favoured at 55°C, which could lead to the observed increase in T_g .

362 In the case of impregnated samples, differences were found in the crystallinity and T_g of the OLE-
363 impregnated samples which suggests that the presence of the extract may be also responsible for the
364 observed changes in these parameters. As shown in Table 1, when compared to the control film,

365 increasing the pressure lowered the % X_c in the PP layer for both modes of impregnation and for both
366 temperature conditions of CO₂ treatment without OLE. However, the presence of the extract did not
367 substantially affect the PET crystallinity. Since the crystallite size rather than the % X_c influences the
368 melting and glass transition temperatures, the scCO₂ process may have a greater influence on the
369 crystallite size of PP in particular.

370 At a pressure of 400 bar, a significant reduction in % X_c is observed as a result of the reorganization of
371 the PP polymer chains caused by the CO₂ sorption at which point CO₂-polymer interactions take place
372 [77]. Moreover, PP chain mobility is favoured in the presence of the extract since the use of co-solvent
373 has been reported to enhance the swelling effect in polymers [21, 78] and a decrease in the crystallinity
374 with the incorporation of other compounds has also been reported in PP [79] and other polymers [80-
375 82]. Since the amorphous regions are increased, mass transfer is favoured [54] thereby increasing the
376 level of impregnation. This was also observed in the present study with regard to the extent of loading
377 (see Figure 1). Although the level of impregnation was measured on the whole film rather than on
378 separate layers, higher pressures generally resulted in a higher AO loading.

379 It was only possible to observe the T_g of the PET layer as the T_g of PP typically occurs at sub-freezing
380 temperatures which are outside the range measurable with the instrument that was used. Generally,
381 supercritical impregnation leads to a decrease in T_g , either due to the swelling effect of CO₂ or the
382 presence of the extract, both of which impart a plasticizing effect [78, 83]. The temperature at which
383 the impregnation process is conducted can therefore have a significant effect on the T_g of the resulting
384 film. In particular, the presence of OLE in samples processed at 55°C contributed to the increase of T_g
385 values previously observed in samples submitted to the CO₂ conditions. This may be due to the
386 increased hydrogen bonding observed in the FTIR analyses [65] (Figure S1) and that may be at a
387 maximum at the higher temperature, which may confirm the hypothesis of the chemical bond between
388 OLE and PET layer.

389 **3.3.2. Thermogravimetric Analysis**

390 As shown in Figure 4, the thermal degradation of the control PET/PP film, and the films subjected to a
391 BM processes with OLE extract occurred over a single step which is confirmed by a single peak in the
392 first derivative curves (see Figure 4). Moreover, there is no separate step that can be attributed to the
393 OLE extract in the thermogravimetric (TG) profile suggesting that these profiles correspond to the
394 degradation of the polymer alone where the multilayer film is behaving as a homogeneous system. In
395 the typical TG profile of the samples used in the current study, there is a significant mass loss
396 commencing at between 300 and 350°C which corresponds to degradation of the polymers and, in all
397 cases, no residual inorganic content was observed after 800°C [84].

398 Kinetic analyses were performed on the thermograms in order to extract the apparent activation energy
399 (E_a) of the degradation step in accordance with the method described by Bigger et al. [51]. The method
400 is based on an iterative computerized technique in which various, well-established models [85-88] are
401 applied to the mass loss curve in order to obtain the best fitting model under the same test conditions
402 and to extract the E_a values. Table 2 shows the results of the TGA fitting analysis and, in general, the
403 fit to the three-dimensional diffusion (D3) and first-order (F1) models are the strongest with the D3
404 model presenting consistently high R^2 values for the fitting parameter for all samples.

405 In the D3 model of decomposition, the expression that describes the model with respect to the degree
406 of conversion, α , is given by [88]:

$$407 \quad g(\alpha) = [1 - (1 - \alpha)^{1/3}]^2 \quad (7)$$

408 The solution of $g(\alpha)$ is a function of the integral, $p(x)$, and therefore a plot of $g(\alpha)$ versus $p(x)$ should
409 give a straight line if the correct model is applied [51]. As shown in Figure 5, a straight line is obtained
410 in the example plot of the sample impregnated by batch mode at 400 bar and 35°C and the R^2 values
411 associated with the measurement of E_a values in Table 2 are consistently high (i.e. > 0.99). With the
412 exception of the sample prepared by the BM process at 55°C and 400 bar, there appears to be an overall
413 trend between the OLE loading (Figure 1) in the samples and the E_a with the observed E_a decreasing
414 with increasing OLE loading. This could be due to the thermal destabilizing effect produced by the low
415 levels of OLE or its degradation products (not detected in the TGA profiles) that are present in the

416 polymer matrices of the laminate film. Furthermore, under certain conditions used in the impregnation
417 process the observed average E_a values are higher than the control film.

418 Table 3 summarises the apparent activation energy values listed in Table 2 in terms of the effects of
419 temperature, pressure and impregnation mode on this parameter. The average apparent E_a values vary
420 from 340 to 385 kJ mol⁻¹ with an E_a value of 372 ± 6 kJ mol⁻¹ obtained for the control film with no
421 treatment. In general, and with the exception of the sample prepared by the BM process at 35°C and
422 400 bar, the upward trend in the observed E_a with increasing % X_c values (see Tables 1 and 2) for those
423 samples prepared at 35°C may be related to the increased stability imparted to the polymer by the
424 increased crystallinity. However, there are several components undergoing pyrolysis including PET,
425 PP, PU adhesive, and OLE with the OLE itself a combination of many compounds. As such, there are
426 many competing processes and there was no general trend observed among the E_a values observed as a
427 result of the different treatments (see Table 3). Any trends amongst the different treatments and
428 conditions would require further investigation to be identified.

429 **3.4. Tensile Strength**

430 Table 4 shows the results of the tensile strength (TS) measurements. Samples subjected to scCO₂
431 treatment at 55°C and either 100 or 400 bar without OLE exhibited higher TS values than those samples
432 processed at 35°C. This elevation in TS with processing temperature was also observed in the cases of
433 samples containing OLE and subjected to BM processing (see Table 4). Upon the addition of OLE the
434 difference in TS resulting from the processing at 55°C and the control was reduced but there is still a
435 significant difference with respect to the 35°C treatment.

436 The results are consistent with the DSC analyses where the T_g values were observed to be higher for
437 samples impregnated at 55°C than at 35°C. This may be due to a hydrogen bonds between PET and
438 OLE which can strengthen the polymer chains and increase the load required to break the polymer film
439 under tension [65] and this is consistent with the findings of the FTIR and DSC analysis. In other
440 systems, the impregnation process has been shown to have little impact on the ductility and mechanical
441 strength of polymer films [89].

442 The impregnation mode was not a significant variable in any of the structural or thermal analyses with
443 the exception of the mechanical properties. Samples impregnated by the SM process had significantly
444 lower tensile break strength ($\alpha = 0.05$) than those impregnated using the BM process. When comparing
445 samples treated at the same temperature and pressure, the continuous flow of the CO₂ under SM had a
446 significant impact on the tensile strength with lower TS values compared to the BM samples. Although
447 the plasticizing effect of the active compounds loaded into the polymer has been reported to affect the
448 mechanical properties [13], in this case the effect of CO₂ appears to be more dominant than the effect
449 of the extract. There was no apparent relationship between the concentration of the extract and the
450 decrease of the tensile strength. This could be due to the low loading of impregnated compounds or the
451 possibility that the OLE is deposited on the surface only. In any case, it is possible that the technique
452 of tensile testing is insufficiently sensitive to detect the slight differences in the TS that may arise at
453 these low levels of loading. Nevertheless, it is clear that the changes in the mechanical properties are
454 not substantial enough as to compromise their use as packaging material. This is in agreement with the
455 results obtained in the supercritical impregnation of other polymers [77].

456 **4. Conclusions**

457 Supercritical impregnation is a very complex process in which the scCO₂-substance-matrix interactions
458 requires optimization of the operational conditions and the method of impregnation. It is clear that the
459 operational conditions will affect polymer films differently depending on their physical and chemical
460 characteristics such as composition, functional groups, thickness and crystallinity. It is therefore critical
461 to evaluate the effect of factors involved in the impregnation processing conditions on key material
462 properties of the film in order to guarantee its integrity after the treatment. In general, the effect of the
463 supercritical treatment was correlated between the FTIR, thermal and mechanical properties analysed.
464 In this study, temperature affected the PP and PET layers differently when CO₂ conditions were applied.
465 Samples treated at 35°C showed lower PP crystallinity due to the higher chain mobility, whereas
466 samples treated at 55°C showed increased T_g for the PET due to the reaction of the carbonyl groups with
467 the scCO₂ under the respective conditions. The FTIR results of the impregnated samples revealed that
468 impregnation occurred in both layers of the film which is an important factor to consider with regard to

469 film orientation. In the presence of OLE, the influence of scCO₂ on the film properties was enhanced,
470 particularly when higher pressures were applied as a result of the favored solubilization of the OLE, the
471 swelling of the PP and the bonding between OLE-PET, thereby favoring the AO loading. Films
472 impregnated at 55°C subsequently showed higher FTIR signals in both layers and higher T_g values than
473 films subjected only to the CO₂ conditions. Conversely, the decrease in crystallinity of PP was favored
474 at higher pressures when the PP chain mobility chain was increased due to the plasticizing effect of the
475 OLE. The mechanical strength was generally stable for samples treated in BM, with those treated in
476 SM showing lower TS values possibly due to the effect of the continuous CO₂ stream applied during
477 impregnation.

478 In general, the best impregnation conditions were obtained at 400 bar and 35°C with a loading rate of
479 2.5 ± 0.4 mg AO/g film. Under these conditions, there is adequate solubility of the OLE, an increase in
480 the amorphous regions of PP and good interactions between PET and OLE. It is possible that in the
481 samples impregnated at 400 bar and 55°C, where the conditions of good solubility and higher
482 amorphous regions in PP are also produced, the hydrogen bonding between PET and OLE is such
483 favored such that migration from the PET layer is limited and subsequent reaction with the DPPH
484 reagent are reduced. In this case, the migration of the compounds should be considered in order to
485 ensure that the packaging film will impart adequate food preservation.

486 The impregnation of natural extracts is also important to optimize given the heterogeneous nature and
487 subsequent solubility of the components. For OLE used in the present study, samples impregnated at
488 100 bar and 35°C and 400 bar and 55°C by SM showed similar AO loadings of 1.8 ± 0.3 and $1.75 \pm$
489 0.01 mg AO/g film respectively.

490 Consideration should therefore be given to the choice of film used for supercritical impregnation only
491 if those changes substantially impact the film properties thereby making it impractical for food
492 packaging purposes. Otherwise, slight modification of the impregnation methods and/or the polymeric
493 substrates may need to be considered in order to obtain effective, active films.

494

495 **5. Acknowledgments**

496 This work is part of a project granted by the Spanish Government (Project CTQ2014-52427-R) through
497 its financing by the FEDER (European Funds for Regional Development). The authors thank the
498 financial support that University of Cadiz which enabled C.C.B. to perform parts of this study abroad,
499 making this collaboration possible.

500 6. References

- 501 [1] B. Marcos, C. Sárraga, M. Castellari, F. Kappen, G. Schennink, J. Arnau, Development of
502 biodegradable films with antioxidant properties based on polyesters containing α -tocopherol and olive
503 leaf extract for food packaging applications, *Food Packag. Shelf Life*, 1 (2014) 140-150.
- 504 [2] L.J. Lu, L.X. Lu, Preparation and properties of quercetin-incorporated high density
505 polyethylene/low density polyethylene antioxidant multilayer film, *Packag. Technol. Sci.*, 31 (2018)
506 433-439.
- 507 [3] C. Zhou, D. Sun, R. Garcia, F.A. Stevie, Determination of chemical composition in multilayer
508 polymer film using ToF-SIMS, *Anal. Methods*, 10 (2018) 2444-2449.
- 509 [4] C. Colin-Chavez, H. Soto-Valdez, E. Peralta, J. Lizardi-Mendoza, R. Balandran-Quintana, Diffusion
510 of natural astaxanthin from polyethylene active packaging films into a fatty food simulant, *Food Res.*
511 *Int.*, 54 (2013) 873-880.
- 512 [5] N.M. Larocca, R.B. Filho, L.A. Pessan, Influence of layer-by-layer deposition techniques and
513 incorporation of layered double hydroxides (LDH) on the morphology and gas barrier properties of
514 polyelectrolytes multilayer thin films, *Surf. Coat. Tech.*, 349 (2018) 1-12.
- 515 [6] A. Cherpinski, S. Torres-Giner, L. Cabedo, J.A. Méndez, J.M. Lagaron, Multilayer structures based
516 on annealed electrospun biopolymer coatings of interest in water and aroma barrier fiber-based food
517 packaging applications, *J. Appl. Polym. Sci.*, 135 (2018).
- 518 [7] X. Zhu, K. Schaich, X. Chen, K. Yam, Antioxidant effects of sesamol released from polymeric films
519 on lipid oxidation in linoleic acid and oat cereal, *Packag. Technol. Sci.*, 26 (2013) 31-38.
- 520 [8] A. Apicella, P. Scarfato, L. Di Maio, L. Incarnato, Transport properties of multilayer active PET
521 films with different layers configuration, *React. Funct. Polym.*, 127 (2018) 29-37.
- 522 [9] E. Joo, Y. Chang, I. Choi, S.B. Lee, D.H. Kim, Y.J. Choi, C.S. Yoon, J. Han, Whey protein-coated
523 high oxygen barrier multilayer films using surface pretreated PET substrate, *Food Hydrocoll.*, 80 (2018)
524 1-7.
- 525 [10] S. Ishtiaque, S. Naz, J. Ahmed, A. Faruqui, Barrier properties analysis of polyethylene
526 terephthalate films (PET) coated with natural Polyphenolic and Gelatin mixture (PGM), *Defect and*
527 *Diffusion Forum*, 382 DDF (2018) 38-43.
- 528 [11] L. Di Maio, F. Marra, T.F. Bedane, L. Incarnato, S. Saguy, Oxygen transfer in co-extruded
529 multilayer active films for food packaging, *AIChE Journal*, 63 (2017) 5215-5221.
- 530 [12] H.J. Jo, K.M. Park, J.H. Na, S.C. Min, K.H. Park, P.S. Chang, J. Han, Development of anti-insect
531 food packaging film containing a polyvinyl alcohol and cinnamon oil emulsion at a pilot plant scale, *J.*
532 *Stored Prod. Res.*, 61 (2015) 114-118.
- 533 [13] J.P. Cerisuelo, R. Gavara, P. Hernández-Muñoz, Natural antimicrobial - Containing EVOH
534 coatings on PP and PET films: Functional and active property characterization, *Packag. Technol. Sci.*,
535 27 (2014) 901-920.
- 536 [14] M.J. Cocero, Á. Martín, F. Mattea, S. Varona, Encapsulation and co-precipitation processes with
537 supercritical fluids: Fundamentals and applications, *J. Supercrit. Fluids*, 47 (2009) 546-555.
- 538 [15] C. Cejudo Bastante, L. Casas Cardoso, C. Mantell Serrano, E.J. Martínez de la Ossa, Supercritical
539 impregnation of food packaging films to provide antioxidant properties, *J. Supercrit. Fluids*, 128 (2017)
540 200-207.
- 541 [16] M. Mulla, J. Ahmed, H. Al-Attar, E. Castro-Aguirre, Y.A. Arfat, R. Auras, Antimicrobial efficacy
542 of clove essential oil infused into chemically modified LLDPE film for chicken meat packaging, *Food*
543 *Control*, 73 (2017) 663-671.

544 [17] K. Simonović, I. Petronijević, D. Kostoski, J. Dojčilović, A.S. Luyt, D. Dudić, Effects of acid
545 treatment at different temperatures on the surface dielectric properties of low-density polyethylene,
546 *Polym. Int.*, 63 (2014) 1924-1929.

547 [18] I. Novák, M. Števiar, A. Popelka, I. Chodák, J. Mosnáček, M. Špírková, I. Janigová, A. Kleinová,
548 J. Sedláček, M. Šlouf, Surface modification of polyethylene by diffuse barrier discharge plasma, *Polym.*
549 *Eng. Sci.*, 53 (2013) 516-523.

550 [19] M.R. Sanchis, V. Blanes, M. Blanes, D. Garcia, R. Balart, Surface modification of low density
551 polyethylene (LDPE) film by low pressure O₂ plasma treatment, *Eur. Polym. J.*, 42 (2006) 1558-1568.

552 [20] Y. Zhao, K. Jung, Y. Shimoyama, Y. Shimogaki, T. Momose, Kinetic effects of methanol addition
553 on supercritical fluid deposition of TiO₂, *J. Supercrit. Fluids*, 138 (2018) 63-72.

554 [21] M. Belizón, M.T. Fernández-Ponce, L. Casas, C. Mantell, E.J. Martínez de la Ossa-Fernández,
555 Supercritical impregnation of antioxidant mango polyphenols into a multilayer PET/PP food-grade film,
556 *J. CO₂ Util.*, 25 (2018) 56-67.

557 [22] M. Champeau, J.M. Thomassin, T. Tassaing, C. Jerome, Drug Loading of Sutures by Supercritical
558 CO₂ Impregnation: Effect of Polymer/Drug Interactions and Thermal Transitions, *Macromol. Mater.*
559 *Eng.*, 300 (2015) 596-610.

560 [23] L.C.S. Herek, R.C. Oliveira, A.F. Rubira, N. Pinheiro, Impregnation of pet films and PHB granules
561 with curcumin in supercritical CO₂, *Braz. J. Chem. Eng.*, 23 (2006) 227-234.

562 [24] K. Miyazaki, I. Tabata, T. Hori, Effects of molecular structure on dyeing performance and colour
563 fastness of yellow dyestuffs applied to polypropylene fibres in supercritical carbon dioxide, *Color.*
564 *Technol.*, 128 (2012) 51-59.

565 [25] D. Sun, R. Zhang, Z. Liu, Y. Huang, Y. Wang, J. He, B. Han, G. Yang, Polypropylene/Silica
566 Nanocomposites Prepared by in-Situ Sol-Gel Reaction with the Aid of CO₂, *Macromol.*, 38 (2005)
567 5617-5624.

568 [26] S.G. Kazarian, Polymer processing with supercritical fluids, *Polym. Sci. - Series C*, 42 (2000) 78-
569 101.

570 [27] E. Kiran, Supercritical fluids and polymers – The year in review – 2014, *J. Supercrit. Fluids*, 110
571 (2016) 126-153.

572 [28] Y. Kong, J.N. Hay, The measurement of the crystallinity of polymers by DSC, *Polym.*, 43 (2002)
573 3873-3878.

574 [29] A. Bouledjoudja, Y. Masmoudi, M. Van Speybroeck, L. Schueller, E. Badens, Impregnation of
575 Fenofibrate on mesoporous silica using supercritical carbon dioxide, *Int. J. Pharm.*, 499 (2016) 1-9.

576 [30] X.-K. Li, H. Lu, G.-P. Cao, Y.-H. Qian, L.-H. Chen, R.-H. Zhang, H.-L. Liu, Y.-H. Shi,
577 Experimental Study of the Synergistic Plasticizing Effect of Carbon Dioxide and Ibuprofen on the Glass
578 Transition Temperature of Poly(methyl methacrylate), *Ind. Eng. Chem. Res.*, 53 (2014) 5873-5885.

579 [31] S. Milovanovic, G. Hollermann, C. Errenst, J. Pajnik, S. Frerich, S. Kroll, K. Rezwani, J. Ivanovic,
580 Supercritical CO₂ impregnation of PLA/PCL films with natural substances for bacterial growth control
581 in food packaging, *Food Res. Int.*, 107 (2018) 486-495.

582 [32] M.A. Fanovich, J. Ivanovic, D. Misic, M.V. Alvarez, P. Jaeger, I. Zizovic, R. Eggers, Development
583 of polycaprolactone scaffold with antibacterial activity by an integrated supercritical extraction and
584 impregnation process, *J. Supercrit. Fluids*, 78 (2013) 42-53.

585 [33] J. Ivanovic, S. Knauer, A. Fanovich, S. Milovanovic, M. Stamenic, P. Jaeger, I. Zizovic, R. Eggers,
586 Supercritical CO₂ sorption kinetics and thymol impregnation of PCL and PCL-HA, *J. Supercrit. Fluids*,
587 107 (2016) 486-498.

588 [34] L. Manna, M. Banchemo, D. Sola, A. Ferri, S. Ronchetti, S. Sicardi, Impregnation of PVP
589 microparticles with ketoprofen in the presence of supercritical CO₂, *J. Supercrit. Fluids*, 42 (2007) 378-
590 384.

591 [35] M.L. Goñi, N.A. Gañán, R.E. Martini, A.E. Andreatta, Carvone-loaded LDPE films for active
592 packaging: Effect of supercritical CO₂-assisted impregnation on loading, mechanical and transport
593 properties of the films, *J. Supercrit. Fluids*, 133 (2018) 278-290.

594 [36] A.M.A. Dias, A. Rey-Rico, R.A. Oliveira, S. Marceneiro, C. Alvarez-Lorenzo, A. Concheiro,
595 R.N.C. Júnior, M.E.M. Braga, H.C. de Sousa, Wound dressings loaded with an anti-inflammatory jucá
596 (*Libidibia ferrea*) extract using supercritical carbon dioxide technology, *J. Supercrit. Fluids*, 74 (2013)
597 34-45.

598 [37] C.V. da Silva, V.J. Pereira, G.M.N. Costa, E.C.M. Cabral-Albuquerque, S.A.B. Vieira de Melo,
599 H.C. de Sousa, A.M.A. Dias, M.E.M. Braga, Supercritical solvent impregnation/deposition of
600 spilanthol-enriched extracts into a commercial collagen/cellulose-based wound dressing, *J. Supercrit.*
601 *Fluids*, 133 (2018) 503-511.

602 [38] J. Sanchez-Sanchez, M.T. Fernández-Ponce, L. Casas, C. Mantell, E.J.M. de la Ossa, Impregnation
603 of mango leaf extract into a polyester textile using supercritical carbon dioxide, *J. Supercrit. Fluids*, 128
604 (2017) 208-217.

605 [39] C. Sharma, R. Dhiman, N. Rokana, H. Panwar, Nanotechnology: An Untapped Resource for Food
606 Packaging, *Front. Microbiol.*, 8 (2017) 1735.

607 [40] G. Amaro-Blanco, J. Delgado-Adámez, M.J. Martín, R. Ramírez, Active packaging using an olive
608 leaf extract and high pressure processing for the preservation of sliced dry-cured shoulders from Iberian
609 pigs, *Innov. Food Sci. Emerg. Technol.*, 45 (2018) 1-9.

610 [41] M. Moudache, C. Nerín, M. Colon, F. Zaidi, Antioxidant effect of an innovative active plastic film
611 containing olive leaves extract on fresh pork meat and its evaluation by Raman spectroscopy, *Food*
612 *Chem.*, 229 (2017) 98-103.

613 [42] A. Mohammadi, S.M. Jafari, A.F. Esfanjani, S. Akhavan, Application of nano-encapsulated olive
614 leaf extract in controlling the oxidative stability of soybean oil, *Food Chem.*, 190 (2016) 513-519.

615 [43] S. Souilem, I. Fki, I. Kobayashi, N. Khalid, M.A. Neves, H. Isoda, S. Sayadi, M. Nakajima,
616 Emerging Technologies for Recovery of Value-Added Components from Olive Leaves and Their
617 Applications in Food/Feed Industries, *Food Bioprocess Tech.*, 10 (2017) 229-248.

618 [44] M. Herrero, T.N. Temirzoda, A. Segura-Carretero, R. Quirantes, M. Plaza, E. Ibañez, New
619 possibilities for the valorization of olive oil by-products, *J. Chromatogr. A*, 1218 (2011) 7511-7520.

620 [45] M.T. Fernández-Ponce, L. Casas, C. Mantell, E. Martínez de la Ossa, Use of high pressure
621 techniques to produce *Mangifera indica* L. leaf extracts enriched in potent antioxidant phenolic
622 compounds, *Innov. Food Sci. Emerg. Technol.*, 29 (2015) 94-106.

623 [46] C. Chinnarasu, A. Montes, M.T. Fernandez-Ponce, L. Casas, C. Mantell, C. Pereyra, E.J.M. de la
624 Ossa, S. Pattabhi, Natural antioxidant fine particles recovery from *Eucalyptus globulus* leaves using
625 supercritical carbon dioxide assisted processes, *J. Supercrit. Fluids*, 101 (2015) 161-169.

626 [47] M. Otero-Pareja, L. Casas, M. Fernández-Ponce, C. Mantell, E. Ossa, Green Extraction of
627 Antioxidants from Different Varieties of Red Grape Pomace, *Molecules*, 20 (2015) 9686.

628 [48] R.L. Blaine, "Thermal Applications Note, Polymer Heats of Fusion", Technical Note TN048,
629 www.tainstruments.com/pdf/literature/TN048.pdf, accessed April, 2017, (2017).

630 [49] A. Pawlak, M. Pluta, J. Morawiec, A. Galeski, M. Pracella, Characterization of scrap poly(ethylene
631 terephthalate), *Eur. Polym. J.*, 36 (2000) 1875-1884.

632 [50] D.C. Bassett, R.H. Olley, On the lamellar morphology of isotactic polypropylene spherulites,
633 *Polym.*, 25 (1984) 935-943.

634 [51] S.W. Bigger, M.J. Cran, I.S.M.A. Tawakkal, Two novel algorithms for the thermogravimetric
635 assessment of polymer degradation under non-isothermal conditions, *Polym. Test.*, 43 (2015) 139-146.

636 [52] M. Champeau, J.M. Thomassin, T. Tassaing, C. Jérôme, Drug loading of polymer implants by
637 supercritical CO₂; assisted impregnation: A review, *J. Control. Release*, 209 (2015) 248-259.

638 [53] C. Cejudo Bastante, L. Casas Cardoso, M.T. Fernández Ponce, C. Mantell Serrano, E.J. Martínez
639 de la Ossa-Fernández, Characterization of olive leaf extract polyphenols loaded by supercritical solvent
640 impregnation into PET/PP food packaging films, *J. Supercrit. Fluids*, 140 (2018) 196-206.

641 [54] J. von Schnitzler, R. Eggers, Mass transfer in polymers in a supercritical CO₂-atmosphere, *J.*
642 *Supercrit. Fluids*, 16 (1999) 81-92.

643 [55] W.L.F. Santos, M.F. Porto, E.C. Muniz, L. Olenka, M.L. Baesso, A.C. Bento, A.F. Rubira,
644 Poly(ethylene terephthalate) films modified with N,N-dimethylacrylamide: Incorporation of disperse
645 dye, *J. Appl. Polym. Sci.*, 77 (2000) 269-282.

646 [56] M. Champeau, J.M. Thomassin, C. Jérôme, T. Tassaing, In situ FTIR micro-spectroscopy to
647 investigate polymeric fibers under supercritical carbon dioxide: CO₂ sorption and swelling
648 measurements, *J. Supercrit. Fluids*, 90 (2014) 44-52.

649 [57] Z. Lei, H. Ohyabu, Y. Sato, H. Inomata, R.L. Smith Jr, Solubility, swelling degree and crystallinity
650 of carbon dioxide-polypropylene system, *J. Supercrit. Fluids*, 40 (2007) 452-461.

651 [58] L. Xie, L. Wei, L. Zhiqing, W. Xiaolin, G. Heling, W. Rongjie, G. Xuhong, L. Cuihua, J. Xin,
652 Underwater polyurethane adhesive with enhanced cohesion by postcrosslinking of glycerol
653 monomethacrylate, *J. Appl. Polym. Sci.*, 135 (2018) 46579.

654 [59] H.F. Shurvell, J.M. Chalmers, *Spectra– Structure Correlations in the Mid- and Far- Infrared*, in:
655 J.M. Chalmers, P.R. Griffith (Eds.) *Handbook of Vibrational Spectroscopy*, Wiley, 2006.

656 [60] M. Champeau, J.M. Thomassin, C. Jerome, T. Tassaing, In situ investigation of supercritical CO₂
657 assisted impregnation of drugs into a polymer by high pressure FTIR micro-spectroscopy, *Analyst*, 140
658 (2015) 869-879.

659 [61] P.W. Labuschagne, M.J. John, R.E. Sadiku, Investigation of the degree of homogeneity and
660 hydrogen bonding in PEG/PVP blends prepared in supercritical CO₂: Comparison with ethanol-cast
661 blends and physical mixtures, *J. Supercrit. Fluids*, 54 (2010) 81-88.

662 [62] R. Abdollahi, M.T. Taghizadeh, S. Savani, Thermal and mechanical properties of graphene oxide
663 nanocomposite hydrogel based on poly (acrylic acid) grafted onto amylose, *Polym. Degrad. Stab.*, 147
664 (2018) 151-158.

665 [63] S. Zhang, R. Li, D. Huang, X. Ren, T.-S. Huang, Antibacterial modification of PET with quaternary
666 ammonium salt and silver particles via electron-beam irradiation, *Mater. Sci. Eng. C*, 85 (2018) 123-
667 129.

668 [64] I.V. Korolkov, Y.G. Gorin, A.B. Yeszhanov, A.L. Kozlovskiy, M.V. Zdorovets, Preparation of
669 PET track-etched membranes for membrane distillation by photo-induced graft polymerization, *Mater.*
670 *Chem. Phys.*, 205 (2018) 55-63.

671 [65] C. Cazan, M. Cosnita, A. Duta, Effect of PET functionalization in composites of rubber–PET–
672 HDPE type, *Arab. J. Chem.*, 10 (2017) 300-312.

673 [66] M.M. Lubna, K.S. Salem, M. Sarker, M.A. Khan, Modification of Thermo-Mechanical Properties
674 of Recycled PET by Vinyl Acetate (VAc) Monomer Grafting Using Gamma Irradiation, *J. Polym.*
675 *Environ.*, 26 (2018) 83-90.

676 [67] F.M. Abdul Aziz, S.N. Surip, N.N. Bonnia, K.A. Sekak, The effect of Pineapple Leaf Fiber (PALF)
677 incorporation into Polyethylene Terephthalate (PET) on FTIR, morphology and wetting properties, in:
678 *IOP Conference Series: Earth and Environmental Science*, 2018.

679 [68] E. Saroufim, C. Celauro, M.C. Mistretta, A simple interpretation of the effect of the polymer type
680 on the properties of PMBs for road paving applications, *Constr. Build Mater.*, 158 (2018) 114-123.

681 [69] S. Milovanovic, D. Markovic, K. Aksentijevic, D.B. Stojanovic, J. Ivanovic, I. Zizovic,
682 Application of cellulose acetate for controlled release of thymol, *Carbohydr. Polym.*, 147 (2016) 344-
683 353.

684 [70] A. López-Periago, A. Argemí, J.M. Andanson, V. Fernández, C.A. García-González, S.G.
685 Kazarian, J. Saurina, C. Domingo, Impregnation of a biocompatible polymer aided by supercritical
686 CO₂: Evaluation of drug stability and drug–matrix interactions, *J. Supercrit. Fluids*, 48 (2009) 56-63.

687 [71] F. Yañez, L. Martikainen, M.E.M. Braga, C. Alvarez-Lorenzo, A. Concheiro, C.M.M. Duarte,
688 M.H. Gil, H.C. de Sousa, Supercritical fluid-assisted preparation of imprinted contact lenses for drug
689 delivery, *Acta Biomater.*, 7 (2011) 1019-1030.

690 [72] A. Rojas, D. Cerro, A. Torres, M.J. Galotto, A. Guarda, J. Romero, Supercritical impregnation and
691 kinetic release of 2-nonanone in LLDPE films used for active food packaging, *J. Supercrit. Fluids*, 104
692 (2015) 76-84.

693 [73] P. Shao, Z. Yan, H. Chen, J. Xiao, Electrospun poly(vinyl alcohol)/permutite fibrous film loaded
694 with cinnamaldehyde for active food packaging, *J. Appl. Polym. Sci.*, 135 (2018).

695 [74] F. López-Saucedo, G.G. Flores-Rojas, J. López-Saucedo, B. Magariños, C. Alvarez-Lorenzo, A.
696 Concheiro, E. Bucio, Antimicrobial silver-loaded polypropylene sutures modified by radiation-grafting,
697 *Eur. Polym. J.*, (2018).

698 [75] S. Molinaro, M. Cruz Romero, M. Boaro, A. Sensidoni, C. Lagazio, M. Morris, J. Kerry, Effect of
699 nanoclay-type and PLA optical purity on the characteristics of PLA-based nanocomposite films, *J. Food*
700 *Eng.*, 117 (2013) 113-123.

701 [76] S.G. Kazarian, M.F. Vincent, F.V. Bright, C.L. Liotta, C.A. Eckert, Specific Intermolecular
702 Interaction of Carbon Dioxide with Polymers, *J. Am. Chem. Soc.*, 118 (1996) 1729-1736.

703 [77] M.L. Goñi, N.A. Gañán, M.C. Strumia, R.E. Martini, Eugenol-loaded LLDPE films with
704 antioxidant activity by supercritical carbon dioxide impregnation, *J. Supercrit. Fluids*, 111 (2016) 28-
705 35.

- 706 [78] Z. Shen, G.S. Huvar, C.S. Warriner, M. Mc Hugh, J.L. Banyasz, M.K. Mishra, CO₂-assisted fiber
707 impregnation, *Polym.*, 49 (2008) 1579-1586.
- 708 [79] D.K. Mandal, H. Bhunia, P.K. Bajpai, A. Kumar, G. Madhu, G.B. Nando, Biodegradation of Pro-
709 oxidant Filled Polypropylene Films and Evaluation of the Ecotoxicological Impact, *J. Polym. Environ.*
710 , 26 (2018) 1061-1071.
- 711 [80] A. Torres, E. Ilabaca, A. Rojas, F. Rodríguez, M.J. Galotto, A. Guarda, C. Villegas, J. Romero,
712 Effect of processing conditions on the physical, chemical and transport properties of polylactic acid
713 films containing thymol incorporated by supercritical impregnation, *Eur. Polym. J.*, 89 (2017) 195-210.
- 714 [81] S.A. Mir, M.A. Shah, B.N. Dar, A.A. Wani, S.A. Ganai, J. Nishad, Supercritical Impregnation of
715 Active Components into Polymers for Food Packaging Applications, *Food Bioprocess Tech.*, 10 (2017)
716 1749-1754.
- 717 [82] C. Villegas, A. Torres, M. Rios, A. Rojas, J. Romero, C.L. de Dicastillo, X. Valenzuela, M.J.
718 Galotto, A. Guarda, Supercritical impregnation of cinnamaldehyde into polylactic acid as a route to
719 develop antibacterial food packaging materials, *Food Res. Int.*, 99 (2017) 650-659.
- 720 [83] M. Jamshidian, E.A. Tehrany, M. Imran, M.J. Akhtar, F. Cleymand, S. Desobry, Structural,
721 mechanical and barrier properties of active PLA-antioxidant films, *J. Food Eng.*, 110 (2012) 380-389.
- 722 [84] M.P. Sepe, *Thermal Analysis of Polymers*, Rapra Technology Limited, 1997.
- 723 [85] D. Dollimore, Thermodynamic, kinetic and surface texture factors in the production of active solids
724 by thermal decomposition, *J. Therm. Anal.*, 38 (1992) 111-130.
- 725 [86] D. Dollimore, T.A. Evans, Y.F. Lee, G.P. Pee, F.W. Wilburn, The significance of the onset and
726 final temperatures in the kinetic analysis of TG curves, *Thermochim. Acta*, 196 (1992) 255-265.
- 727 [87] D. Dollimore, T.A. Evans, Y.F. Lee, F.W. Wilburn, Correlation between the shape of a TG/DTG
728 curve and the form of the kinetic mechanism which is applying, *Thermochim. Acta*, 198 (1992) 249-
729 257.
- 730 [88] D. Dollimore, The application of thermal analysis in studying the thermal decomposition of solids,
731 *Thermochim. Acta*, 203 (1992) 7-23.
- 732 [89] M.L. Goñi, N.A. Gañán, S.E. Barbosa, M.C. Strumia, R.E. Martini, Supercritical CO₂-assisted
733 impregnation of LDPE/sepiolite nanocomposite films with insecticidal terpene ketones: Impregnation
734 yield, crystallinity and mechanical properties assessment, *J. Supercrit. Fluids*, 130 (2017) 337-346.

735

736

737

738

Table 1. Values of T_m , $\%X_c$, T_g , and T_{cc} obtained from DSC thermograms of control (untreated) PET/PP laminate films, films treated with CO₂ and

739

impregnated films with OLE.

Mode	Sample	PP		PET			
		$T_m/^\circ\text{C}$	$\%X_c$	$T_g/^\circ\text{C}$	$T_{cc}/^\circ\text{C}$	$T_m/^\circ\text{C}$	$\%X_c$
	Control	161.60 ± 0.59	35.95 ± 0.32	82.70 ± 0.28	223.23 ± 5.07	253.30 ± 0.23	29.59 ± 0.47
No Extract (BM)	100 bar, 35°C	161.72 ± 0.11	31.02 ± 1.70	82.20 ± 0.42	227.21 ± 0.64	253.33 ± 0.02	28.81 ± 1.08
	400 bar, 35°C	161.85 ± 0.23	30.93 ± 2.93	82.85 ± 0.49	225.71 ± 1.41	253.14 ± 0.19	30.96 ± 2.97
	100 bar, 55°C	161.12 ± 0.08	35.37 ± 1.42	90.08 ± 1.24	223.75 ± 0.85	253.31 ± 0.43	29.66 ± 1.47
	400 bar, 55°C	161.46 ± 0.09	36.26 ± 1.72	93.63 ± 7.81	222.15 ± 2.84	253.24 ± 0.38	28.68 ± 0.21
BM	100 bar, 35°C	160.60 ± 0.93	35.12 ± 1.13	82.85 ± 0.07	231.18 ± 0.99	253.07 ± 0.15	26.55 ± 3.28
	400 bar, 35°C	163.03 ± 0.87	28.85 ± 1.26	83.06 ± 0.93	233.11 ± 1.70	254.13 ± 0.24	29.16 ± 3.69
	100 bar, 55°C	160.87 ± 0.47	35.25 ± 1.70	96.39 ± 1.85	230.41 ± 4.59	252.64 ± 0.73	29.34 ± 0.79
	400 bar, 55°C	161.78 ± 1.01	33.57 ± 3.04	97.30 ± 1.27	220.97 ± 2.53	252.46 ± 0.76	31.14 ± 2.25
SM	100 bar, 35°C	161.38 ± 0.26	30.58 ± 4.39	102.45 ± 3.32	228.50 ± 1.45	253.31 ± 0.43	28.72 ± 6.16
	400 bar, 35°C	162.19 ± 0.70	30.15 ± 1.74	83.28 ± 0.33	229.75 ± 1.27	253.96 ± 0.43	25.50 ± 2.61
	100 bar, 55°C	161.56 ± 0.79	32.66 ± 2.54	95.22 ± 3.27	227.71 ± 4.61	252.73 ± 0.17	30.63 ± 1.55
	400 bar, 55°C	161.98 ± 0.35	31.61 ± 1.29	86.75 ± 0.07	222.51 ± 0.22	253.08 ± 0.11	27.93 ± 2.14

740

741 **Table 2.** Values of the kinetic model fitting parameter, ρ , linear regression coefficient, R^2 , and apparent activation energies, E_a , for the thermal decomposition
 742 of PET/PP laminate films subjected to scCO₂ impregnation with and without OLE and under BM or SM conditions (degree of conversion range: $0.1 \leq \alpha \leq 0.9$).

	Control	No extract (BM)				SM				BM			
Kinetic Model		100 bar 35°C	100 bar 55°C	400 bar 35°C	400 bar 55°C	100 bar 35°C	100 bar 55°C	400 bar 35°C	400 bar 55°C	100 bar 35°C	100 bar 55°C	400 bar 35°C	400 bar 55°C
Acceleratory													
Pn Power law	0	0	0	0	0	0	0.001	0	0	0.006	0	0	0
E1 Exponential law	0.517	0.516	0.517	0.516	0.518	0.518	0.518	0.516	0.516	0.518	0.518	0.519	0.516
Sigmoidal													
A2 Avrami-Erofeev	0.781	0.713	0.740	0.730	0.775	0.683	0.736	0.706	0.686	0.733	0.733	0.775	0.714
A3 Avrami-Erofeev	0.760	0.693	0.704	0.710	0.742	0.649	0.716	0.687	0.651	0.711	0.707	0.745	0.686
A4 Avrami-Erofeev	0	0	0	0	0	0	0	0	0	0	0	0	0
B1 Prout-Tompkins	0	0	0	0	0	0	0	0	0	0	0	0	0
Deceleratory													
<i>Geometrical</i>													
R2 Contracting area	0.829	0.795	0.814	0.800	0.844	0.808	0.880	0.820	0.767	0.876	0.855	0.854	0.817
R3 Contracting volume	0.873	0.873	0.893	0.864	0.895	0.856	0.872	0.872	0.866	0.874	0.891	0.900	0.889
<i>Diffusion</i>													
D1 One dimensional	0.597	0.545	0.567	0.556	0.609	0.621	0.671	0.575	0.506	0.659	0.610	0.618	0.566
D2 Two dimensional	0.930	0.936	0.940	0.934	0.938	0.960	0.984	0.958	0.936	0.981	0.961	0.943	0.954
D3 Three dimensional	0.986	0.995	0.998	0.980	0.984	0.945	0.955	0.982	0.959	0.959	0.982	0.987	0.991
D4 Ginstling-Brounshtein	0.947	0.959	0.962	0.956	0.957	0.956	0.976	0.982	0.958	0.984	0.978	0.960	0.977
<i>Reaction Order</i>													
F1 First order	0.989	0.958	0.976	0.970	0.995	0.908	0.919	0.944	0.961	0.923	0.949	0.973	0.958
F2 Second order	0.889	0.862	0.871	0.874	0.877	0.784	0.798	0.835	0.864	0.803	0.836	0.868	0.848
F3 Third order	0.655	0.639	0.649	0.648	0.643	0.540	0.538	0.603	0.656	0.547	0.597	0.631	0.621
D3 model E_a /kJ mol ⁻¹	372 ± 6.1	370 ± 9.6	353 ± 0.2	348 ± 3.3	340 ± 0.6	355 ± 4.8	382 ± 0.2	378 ± 2.6	352 ± 1.2	379 ± 0.4	385 ± 0.4	358 ± 1.0	385 ± 1.1
$g(\alpha)$ vs. $p(x)$ R^2	0.9999	0.9982	0.9999	0.9996	0.9982	0.9995	0.9996	0.9991	0.9987	0.9937	0.9987	0.9998	0.999

Table 3. Average values of apparent activation energies, E_a , for the thermal decomposition of PET/PP laminate films subjected to different treatments. The control is the untreated film.

Treatment	Average E_a value/kJ mol⁻¹
Control	372 ± 6.1
Temperature	
35°C	365 ± 3.6
55°C	366 ± 0.6
Pressure	
100 bar	371 ± 2.6
400 bar	360 ± 1.6
Mode	
SM	367 ± 2.2
BM	377 ± 0.7
No OLE (BM)	353 ± 3.4

Table 4. Tensile strength results of control and impregnated PET/PP laminate films subjected to different treatments.

Mode	Sample	Tensile Strength/kN
	Control	56.5 ± 8
No extract (BM)	100 bar, 35°C	55.4 ± 3.0
	400 bar, 35°C	52.4 ± 4.2
	100 bar, 55°C	62.5 ± 3.1
	400 bar, 55°C	61.5 ± 1.3
BM	100 bar, 35°C	57.1 ± 1.1
	400 bar, 35°C	59.6 ± 2.3
	100 bar, 55°C	65.3 ± 3.9
	400 bar, 55°C	66.5 ± 8.2
SM	100 bar, 35°C	48.6 ± 2.5
	400 bar, 35°C	48.6 ± 4.2
	100 bar, 55°C	54.5 ± 4.9
	400 bar, 55°C	54.3 ± 4.4

*Films treated with CO₂ (no extract) were processed by BM

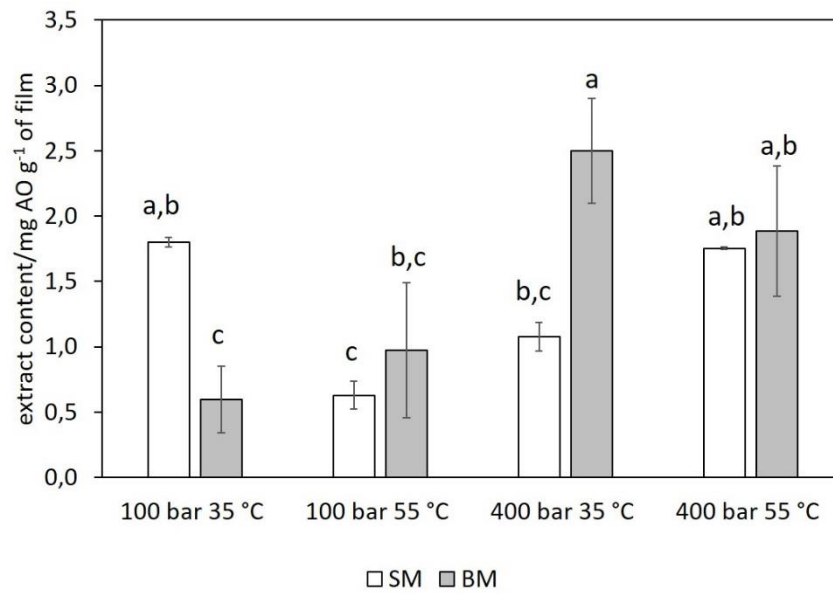
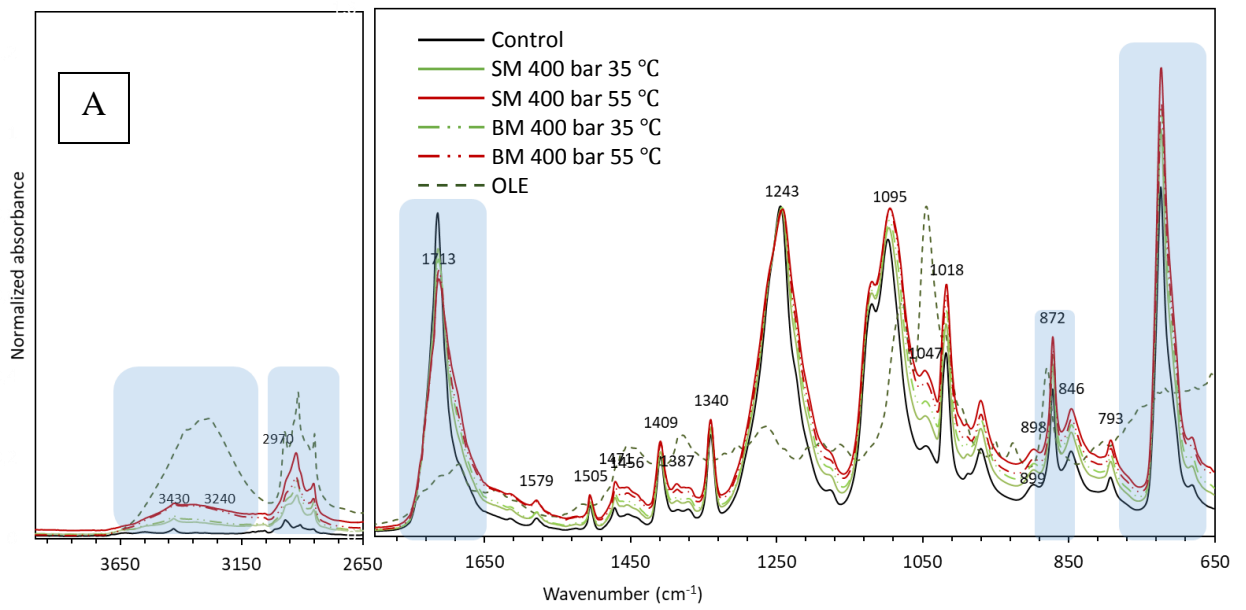
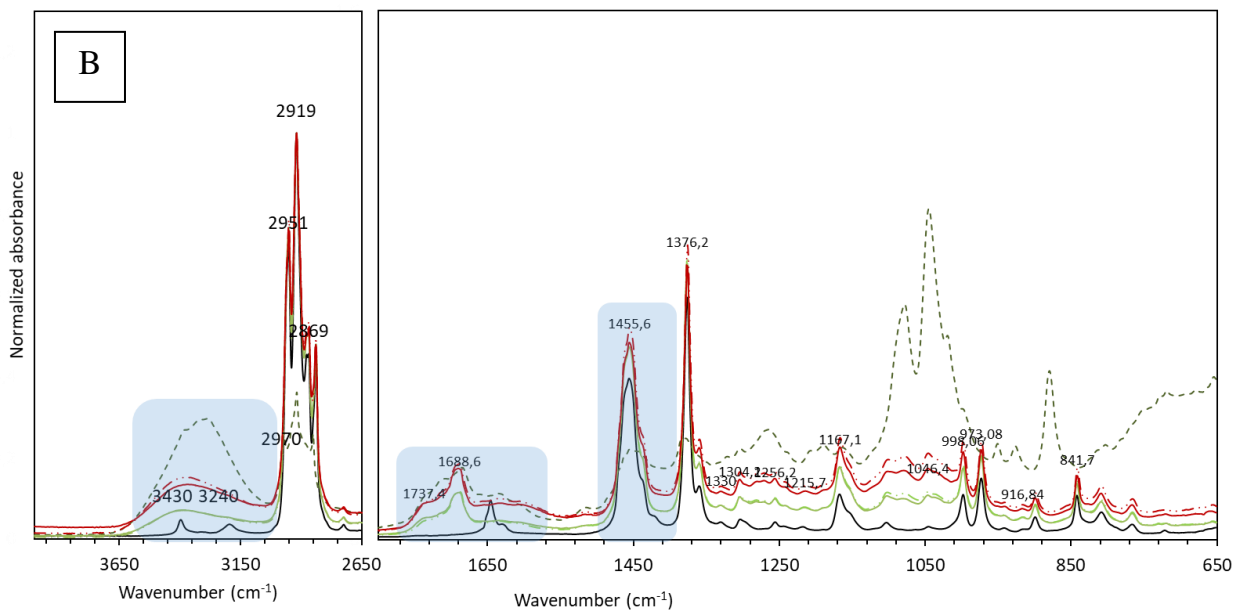


Figure 1. Antioxidant loading in PET/PP laminate films impregnated by the SM and BM processes ($n = 3$). Letters show statistical differences among samples ($\alpha = 0.05$).



1



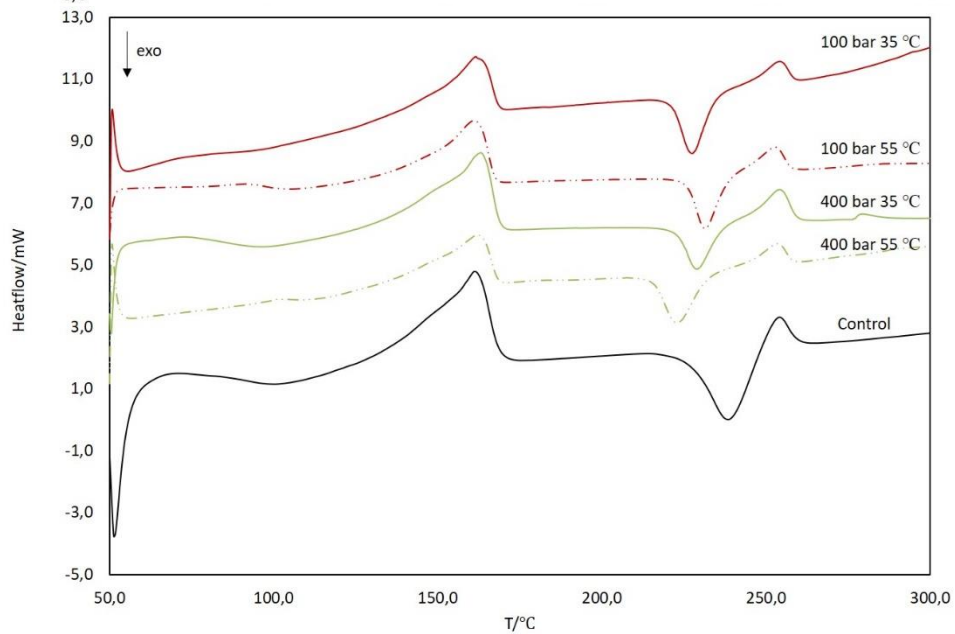
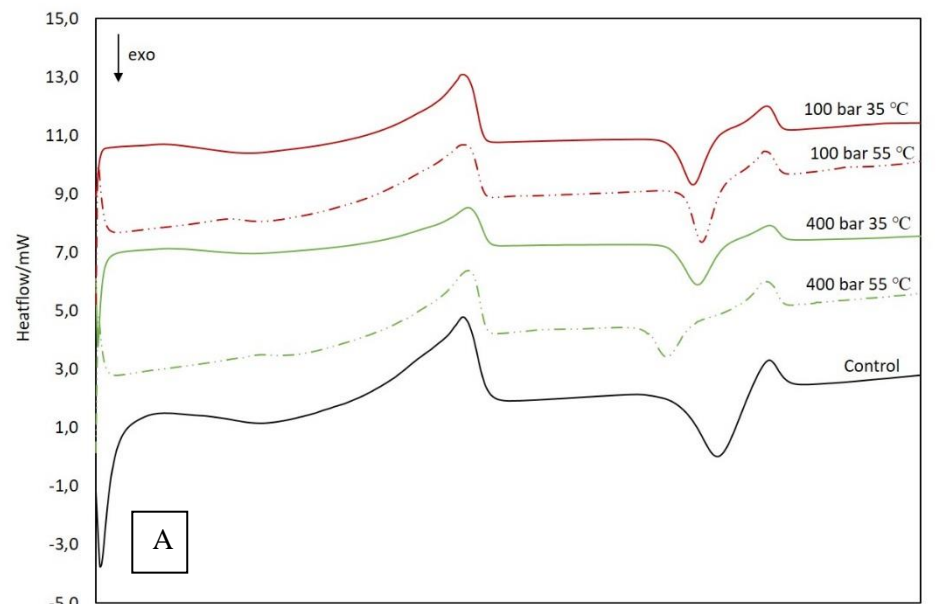
2

3

4 Figure 2. FTIR-ATR spectra of PET/PP laminate film impregnated with OLE at 400 bar: (A) PET
 5 layer and (B) PP layer.

6

7

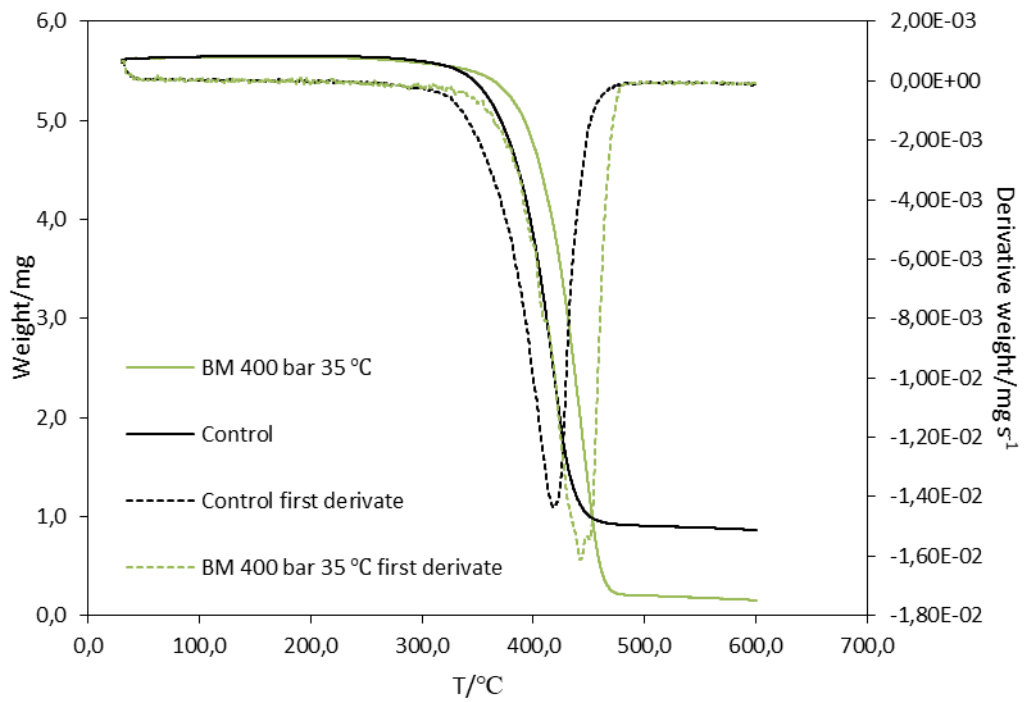


B

17 * The control sample is referred to the non-treated film

18 Figure 3. DSC thermograms of PET/PP laminate film samples impregnated by: (A) SM and (B)
 19 BM. The control sample is non-treated film.

20



21

22 Figure 4. TGA thermograms and first derivative plots of control sample (non-treated PET/PP
 23 multilayer film) and PET/PP laminate film impregnated with OLE by the BM process at 400 bar
 24 and 35°C.

25

26

27

28

29

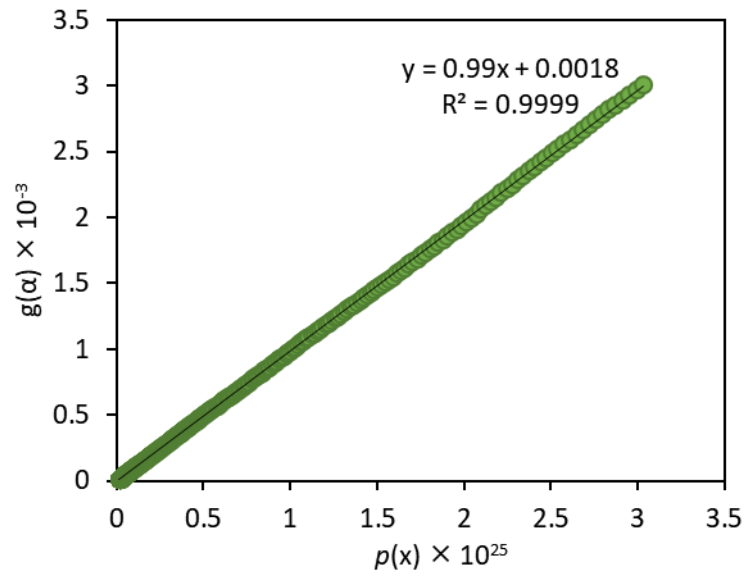
30

31

32

33

34



35

36 Figure 5. Plots of $g(\alpha)$ versus $p(x)$ for the three-dimensional diffusion (D3) fitting of PET/PP
37 laminate film sample impregnated with OLE by the BM process at 400 bar and 35°C.

38

39

40